Kinematics and Design of a New Leg Exoskeleton for Human Motion Assistance

Geonea Ionut(✉), Nicolae Dumitru, Cristian Copilusi, Laura Grigorie, and Daniela Tarnita

Faculty of Mechanics, University of Craiova, Craiova, Romania
igeonea@yahoo.com

Abstract. In this paper there are two original solutions for mechanisms usable in exoskeleton systems for assisting human locomotion. The solutions presented are based on closed cinematic chains containing pantograph mechanisms. A biomechanical analysis of human walking is performed on a healthy subject. Thus, the motion laws of human legs are obtained, that will be compared to those made by the exoskeleton leg. To study the movement of the exoskeleton, a kinematic model is developed for the situation when the mechanism operates on a supporting base. Based on the virtual model, simulation of the exoskeleton's motion on ground is performed. The motion laws obtained for the exoskeleton are compared to those obtained for humans.

Keywords: Human leg · Motion assistance · Exoskeleton design · Kinematics

1 Introduction

The purpose of this paper is to present a mechanism for the leg of an exoskeleton designed to assist human walking and rehabilitation. There are presented two mechanisms solutions that have in the structure 5 and 7 kinematic elements, and a single motor element. Both solutions are original and are developed by the authors. The first solution was presented at the IFToMM 2019 World Congress [1] and the second solution is not presented at any scientific event. Of the two, the best solution for assisting movement is the second, and this will be the subject of this study. The idea of developing exoskeleton systems is directed in two major directions [2–5]. In the first direction, open kinematic chains are used which have motor movements in the joints. These systems are very developed, the achievements of such rehabilitation systems are presented in review studies [6, 7]. The second direction is based on the development of mobile systems based on closed cinematic chains, which have a human foot-like structure. Usually these solutions need one actuator, being single DOF [5, 8–12]. The second direction has several advantages, among which we mention: it uses an actuator, so it is simpler and cheaper; the transmitted forces are amplified by the closed kinematic chain; can be adapted to patients of varying sizes.

The subject of development of exoskeleton systems is of particular importance in the field of medical rehabilitation: in the field of machine building are executed exoskeleton

M. A. Laribi et al. (Eds.): MeTrApp 2023, MMS 124, pp. 199–208, 2023.
https://doi.org/10.1007/978-3-031-29815-8_20

type robots to help operators in the band; in the field of augment of the movement; to humanoid robots.

In this paper two exoskeleton leg solution are proposed. The novel solutions are based on a closed loop kinematic chain linkage. A kinematic study of the human movement is being carried out to compare the movement of the exoskeleton. The exoskeleton solution is built in the Solid Works virtual environment. Based on this virtual model, the exoskeleton motion will be studied with the ADAMS software. The results obtained in simulating the movement of the exoskeleton are compared with those of human walking. The mean values of the hip and knee motion amplitude of the exoskeleton are close to those of the human.

2 Human Gait Experimental Study

For human gait experimental study [13, 14], a Biometrics measurements system based on electro-goniometers is used. Experimental data acquired for normal walking during 40 s from a 34 years old healthy subject are reported with plots as angle variation in time, for the ankle, knee, and hip joints, both in sagittal and frontal plane, (Fig. 1).

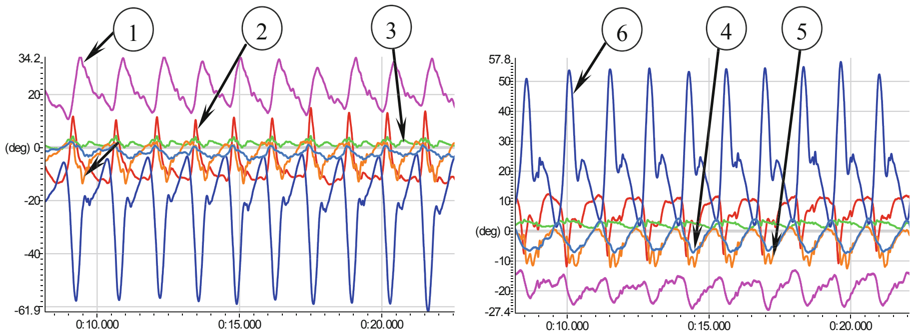

Fig. 1. Healthy human measured joints angle, in sagittal and frontal plane, for left leg and for right leg.

The experimental data shown in Fig. 1 are obtained using the Biometrics Equipment. This equipment is equipped with electro-goniometer type sensors, which are mounted on the joints of the human foot by soldering. A sensor records the flexion-extension angle in the sagittal plane, as well as angles in the frontal plane, being coupled with a device, which transmits the data via Bluetooth to a laptop computer. Human gait shows variability from subject to subject, or even within the same individual from one step to the next. In order to obtain representative results, for the collected data stream we processed to obtain the average cycle of variation of the angles in the leg joints. These data can also be collected with another type of instrument [14], and are necessary for the design of the exoskeleton as well as for the analysis of its performance. With the help of Biometrics software and goniometer sensors, the angular variations of each joint were acquired and plotted, where the plots represent the following: 1-hip flexion/extension; 2-ankle plantar flexion/dorsi flexion; 3 – hip abduction/adduction; 4 – ankle inversion/eversion; 5-knee valgus/varus; 6-knee flexion/extension. The knee flexion extension angle amplitude reaches 60°, as is plotted in Fig. 1, and the hip joint flexion extension angle amplitude reaches 35–40°, as is plotted in same figure.

3 Leg Exoskeleton Mechanism Design

Two original kinematic schemes are proposed. As a result of the kinematic study, the second scheme is suitable for assisting human locomotion, since the movements of the second one is closer to those of a normal human walking. The kinematics scheme of the mechanisms for the assistant's exoskeleton legs are shown in Fig. 2. The proposed leg mechanism is composed by a pantograph mechanism completed with a Chebyshev mechanism for the first one. For the second solution the structure is simplified with a pantograph mechanism and one actuator placed on the link (3).

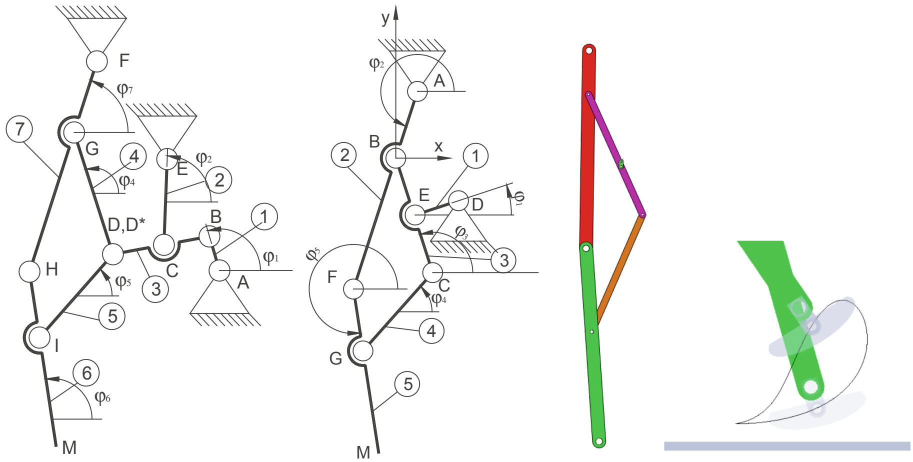

Fig. 2. Kinematics scheme of the proposed legs mechanisms and design model in Solid Works.

The links are noted with digits from (1) to (5–7) and the joints with letters. The motor link of the mechanism is denoted with (1). For the second solution the link (2) represents the femur and the tibia link is (5). Also, the joint A represents the hip joint, and the knee joint is noted with F. The size of the links (2) and (5) can be adjusted so that the shape of the point M trajectory to be an ovoid one, as to human gait.

This leg mechanism can assure the mobility of knee and hip joints. The ankle joint it is not considered because of design solution simplicity.

4 The Kinematic Analysis

A theoretical analysis of the leg exoskeleton kinematics was performed in order to evaluate and simulate performances and operation. The point M position, reported to the

XY reference system, Fig. 2, is evaluated as a function of input angle φ_1 and dimensional parameters of the linkage. Geometrical parameters are presented in Fig. 2.

The calculation of the degree of mobility is done with the relation:

$M = 3n - 2c_5 - c_4 = 1$, so, the actuator is the link 1.

The input data are known as the lengths of the elements and the coordinates of the fixed joints:

- the links length: $l_{DE} = 12.5$ mm, $l_{AB} = 100$ mm, $l_{AF} = 450$ mm, $l_{FM} = 440$ mm, $l_{FG} = 190$ mm, $l_{CG} = 290$ mm, $l_{BE} = 180$ mm, $l_{CE} = 120$ mm, $l_{BC} = 300$ mm.
- the coordinates of the rotation joint to basis have the values: $x_D = 71$ mm, $y_D = -252$ mm. $x_A = y_A = 0$.
- law of motion for driving link: $\omega_1 = 3\,\text{rad/s}$.

The sizes of the elements are set according to the size of the human subject, who will be given assistance when walking. Elements 2 and 5, which structurally model the femur and tibia of the human foot, shall be made in a modular construction allowing their length to be modified within certain limits. The lengths of the other elements were derived from the dimensional synthesis of the mechanism, which was carried out in the first phase using 3D design and motion simulation techniques available in Solid Works.

We write the position equations to calculate the joints coordinates. For link 1, we have:

$$\begin{cases} x_E = x_D + l_{DE} \cdot \cos\varphi_1 \\ y_E = y_D + l_{DE} \cdot \sin\varphi_1 \end{cases} \tag{1}$$

For the structural Assur group EAB we known, the rotation joints coordinates: $x_A = y_A = 0$ and x_E, y_E that are known from Eq. (1).

The position equations for joint B are:

$$\begin{cases} x_B = x_A + l_{AB} \cdot \cos\varphi_2 = x_E + l_{BE} \cdot \cos\varphi_3 \\ y_B = y_A + l_{AB} \cdot \sin\varphi_2 = y_E + l_{BE} \cdot \sin\varphi_3 \end{cases} \tag{2}$$

In order to compute the variation of the angle the terms that contain the other unknown are isolated, as in Eq. (3):

$$\begin{cases} l_{AB} \cdot \cos\varphi_2 = (x_E - x_A) + l_{BE} \cdot \cos\varphi_3 \\ l_{AB} \cdot \sin\varphi_2 = (y_E - y_A) + l_{BE} \cdot \sin\varphi_3 \end{cases} \tag{3}$$

The following notations of the terms, is used: $(x_E - x_A) = a_1$, $(y_E - y_A) = a_2$.

We square up and sum the equations of the system (3), and the Eq. (4) is obtained:

$$l_{AB}^2 = a_1^2 + a_2^2 + l_{BE}^2 + 2a_1 l_{BE} \cdot \cos\varphi_3 + 2a_2 l_{BE} \sin\varphi_3 \tag{4}$$

The Eq. (4) is a trigonometric equation with nonlinear coefficients of the form:

$$A_3 \cdot \sin\varphi_3 + B_3 \cdot \cos\varphi_3 + C_3 = 0 \tag{5}$$

The solutions of Eq. (5) are:

$$\varphi_3 = 2\tan^{-1}\frac{A_3 \pm \sqrt{A_3^2 + B_3^2 - C_3^2}}{B_3 - C_3} \tag{6}$$

where:

$$A_3 = -2a_2 l_{BE},\ B_3 = -2a_1 l_{BC},\ C_3 = l_{AB}^2 - a_1^2 - a_2^2 - l_{BE}^2. \tag{7}$$

To calculate the variation of the angle φ_2 the procedure is as follows:

$$\begin{cases} l_{BE} \cdot \cos\varphi_3 = (x_A - x_E) + l_{AB}\cos\varphi_2 \\ l_{BE} \cdot \sin\varphi_3 = (y_A - y_E) + l_{AB}\sin\varphi_2 \end{cases} \tag{8}$$

With the notations: $(x_A - x_E) = -a_1$, $(y_A - y_E) = -a_2$, the equations of system (8) are squared and summed, resulting:

$$l_{BE}^2 = a_1^2 + a_2^2 + l_{AB}^2 - 2a_1 l_{AB} \cdot \cos\varphi_2 - 2a_2 l_{AB}\sin\varphi_2 \tag{9}$$

The solutions of Eq. (9) are:

$$\varphi_2 = 2\tan^{-1}\frac{A_2 \pm \sqrt{A_2^2 + B_2^2 - C_2^2}}{B_2 - C_2} \tag{10}$$

where: $A_2 = 2a_2 l_{AB},\ B_2 = 2a_1 l_{AB},\ C_2 = l_{BE}^2 - a_1^2 - a_2^2 - l_{AB}^2$.

For the structural Assur group FGC, are known: the coordinates x_F, y_F, x_C, y_C.

The position equation for the joint G is:

$$\begin{cases} x_G = x_F + l_{FG} \cdot \cos\varphi_5 = x_C + l_{CG} \cdot \cos\varphi_4 \\ y_G = y_F + l_{FG} \cdot \sin\varphi_5 = y_C + l_{CG} \cdot \sin\varphi_4 \end{cases} \tag{11}$$

In order to compute the angle φ_4 are grouped the terms like in Eq. (12):

$$\begin{cases} l_{FG}\cos\varphi_5 = (x_G - x_F) + l_{CG} \cdot \cos\varphi_4 \\ l_{FG}\sin\varphi_5 = (y_G - y_F) + l_{CG} \cdot \sin\varphi_4 \end{cases} \tag{12}$$

We make the notations: $(x_G - x_F) = a_3$, $(y_G - y_F) = a_4$. The equations of system (12), after square up and sum are:

$$l_{FG}^2 = a_3^2 + a_4^2 + l_{CG}^2 + 2a_c l_{CG} \cdot \cos\varphi_4 + 2a_4 l_{CG}\sin\varphi_4 \tag{13}$$

The solutions of Eq. (13) are:

$$\varphi_4 = 2\tan^{-1}\frac{A_4 \pm \sqrt{A_4^2 + B_4^2 - C_4^2}}{B_4 - C_4} \tag{14}$$

where: $A_4 = -2a_4 l_{CG},\ B_4 = -2a_3 l_{CG},\ C_4 = l_{FG}^2 - a_3^2 - a_4^2 - l_{CG}^2$. To calculate the variation of the angle φ_5 the terms of Eq. (12) are grouped as in Eq. (15):

$$\begin{cases} l_{CG} \cdot \cos\varphi_4 = (x_F - x_C) + l_{FG}\cos\varphi_5 \\ l_{CG} \cdot \sin\varphi_4 = (y_F - y_C) + l_{FG}\sin\varphi_5 \end{cases} \tag{15}$$

With the notations: $(x_F - x_C) = -a_3$, $(y_F - y_C) = -a_4$, the equations of system (15) are square up and summed. Solutions of Eq. (15) are:

$$\varphi_5 = 2\tan^{-1}\frac{A_5 \pm \sqrt{A_5^2 + B_5^2 - C_5^2}}{B_5 - C_5} \tag{16}$$

where: $A_5 = 2a_4 l_{FG},\ B_5 = 2a_3 l_{FG},\ C_5 = l_{CG}^2 - a_3^2 - a_4^2 - l_{FG}^2$.

By numerical processing of the kinematic equations, we presented in Figs. 3, 4 and 5 the laws of variation of the angles of position of kinematic elements and point M motion. Kinematic equations above correspond to the situation when the mechanism works on a base support. In Figs. 3 and 4 is plotted the angular variation computed for the exoskeleton links position angles. The translational displacement of the point M is presented in Fig. 5.

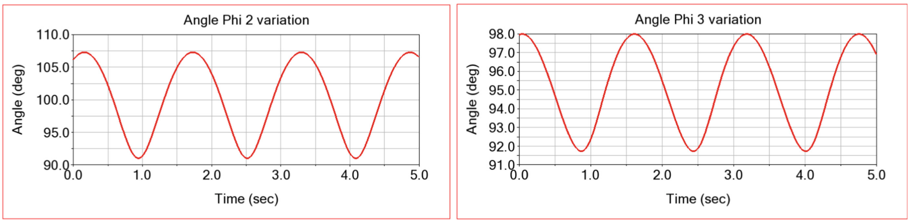

Fig. 3. Time variation of the angle Phi 2 and Phi 3.

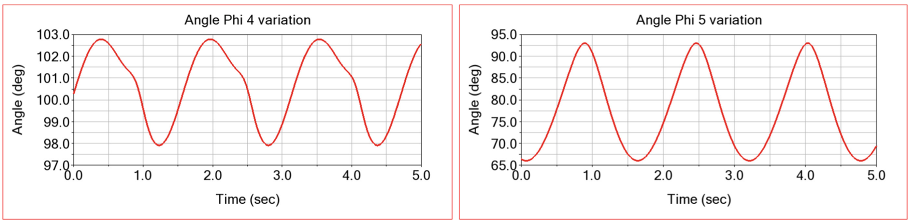

Fig. 4. Time variation of the angle Phi 4 and Phi 5.

The computed angular variation for Phi 2, from Fig. 3 follows the limits obtained from experimental research of human gait for the hip joint. For hip joint this limit is between 0 and 18° for the exoskeleton and 25° for human. For knee joint this limit is between 0 and 30° for the exoskeleton leg and 50° for human leg. It can be observed that the computed values are similar in case of human gait analysis and computed values from kinematics.

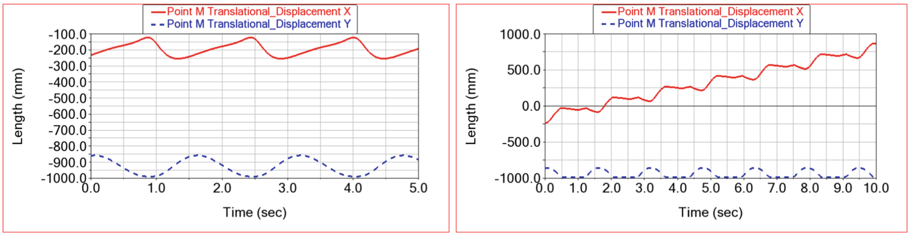

Fig. 5. Point M position upon X and Y axis.

5 Design of CAD Model and Dynamic Simulation

A mechanical design of a proposed exoskeleton is represented in Fig. 6. The structure must be designed to permit adjustments of mechanism links in accordance with different human body constitution. A dynamic simulation has been developed by using a proper model for operation in ADAMS environment (ADAMS 2020). Contact stiffness, damping coefficients, and friction force coefficients have been defined accordingly as listed in Table 1 with links made of steel. The exoskeleton consists of two mechanisms for the left and right legs. The legs are composed of 5 elements connected by 7 kinematic revolute joints. The electric motor with reducer (6), which is mounted on the upper frame (7), is used to drive the two mechanisms, with a chain transmission.

In Fig. 6 we have kept the numbering of the kinematic elements as in Fig. 2, as well as the notations indicated for the kinematic joints of the leg mechanism.

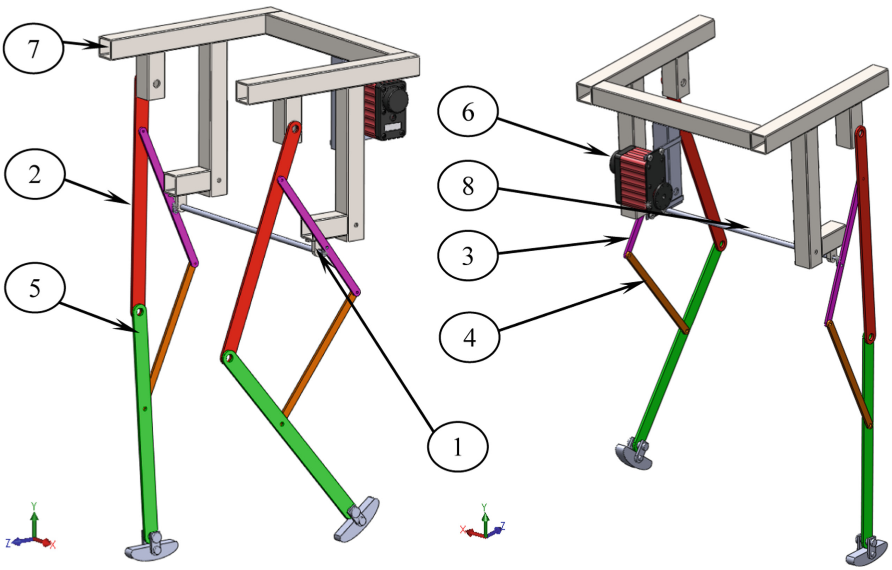

Fig. 6. A mechanical design of the proposed exoskeleton.

By means of a chain wheel drive transmission, the movement is transmitted to the shaft (8), which is mounted on the upper frame (7) by means of radial-axial ball bearings. The motor elements (1) of the two leg mechanisms are connected to the drive shaft (8) and are oriented to 180°. On the upper frame, the links (1) and (2) are connected by means of the rotation joints (with bolts) A and D. The exoskeleton leg is designed with a human leg-like structure: the joint (A) represents the hip joint, the joint (F) represents the knee joint and the (AF) and the (FM) segments represent the femur and the tibia segments of the human leg.

Table 1. ADAMS parameters used for dynamic simulation.

Parameter	Value	Parameter	Value
Elasticity modulus	2.1·105 N/mm^2	Friction force, μs	0.4
Density	7.8·10^{-6} kg/mm^3	Contact force exponent	1.2
Penetration depth	0.1 mm	Damping; Stiffness	400 Ns/mm; 1200 N/mm

The simulation settings for the leg exoskeleton are considered like those in real conditions. The exoskeleton virtual model has been positioned in biped locomotion position when the right leg touches the ground and the left leg is in swing phase. This is the same initial position of the human subjected to experimental gait study. Computed exoskeleton walking sequences are represented in Fig. 7, 8 and main kinematic parameters are depicted with plots in Figs. 3, 4 and 5. From Figs. 3 and 4 it can be concluded that

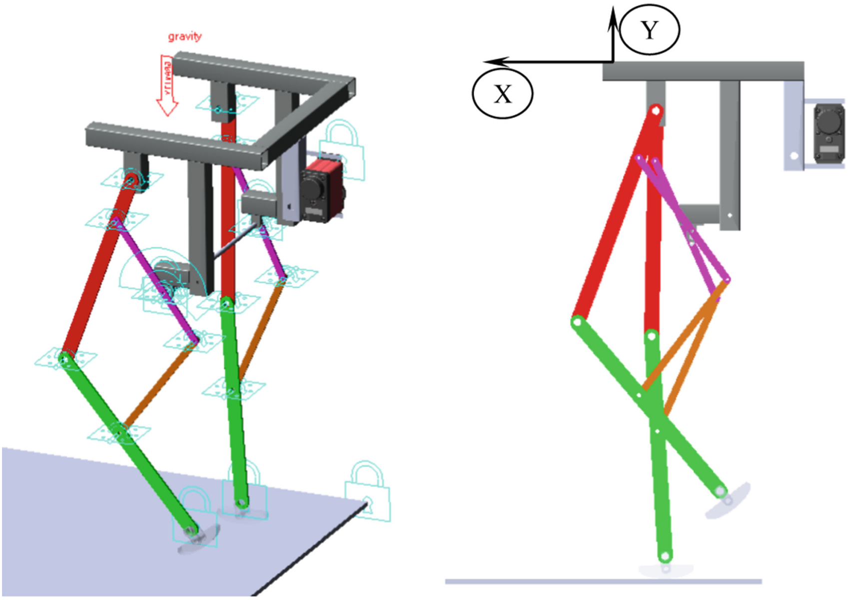

Fig. 7. ADAMS simulation model of the exoskeleton.

the exoskeleton hip and knee joints angular variations are comparable with those from experimental human gait motion analysis.

A sequence of gait stances achieved by the leg is shown in Fig. 8. Also is depicted the ovoid trajectory of the leg when she operates on a fixed support.

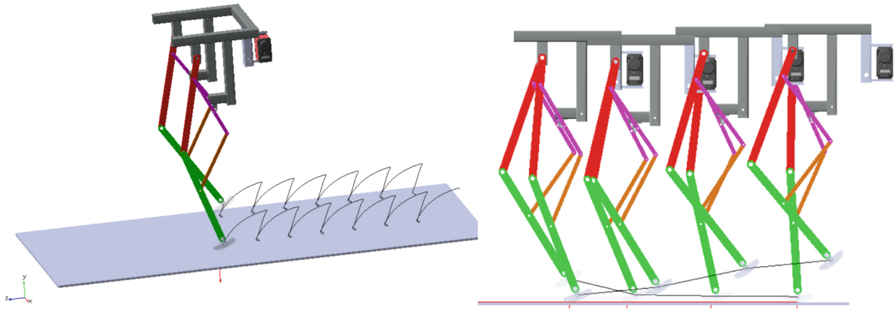

Fig. 8. A walking frames in ADAMS simulation of the exoskeleton.

6 Conclusions

A new exoskeleton leg mechanism is presented, with computer design model, simulation results and discussion. There are two similar kinematic schemes as a solution for the exoskeleton system, which contain a pantograph mechanism in the structure. The kinematic analysis of human walking has highlighted the motion laws of the leg joints. The idea behind the mechanism was the human-like structure. Of the two mechanisms presented, the second structure realizes motion laws close to humans. For this purpose, comparative analysis of motion laws between human and exoskeleton was performed using the second structure. The exoskeleton system presented can be improved by building an adjustable model on patients' dimensions. Simulation results obtained are comparable as angular amplitude, with results obtained on human healthy subjects.

References

1. Geonea, I., Dumitru, N., Tarnita, D., Rinderu, P.: Design and kinematics of a new leg exoskeleton for human motion assistance. In: Advances in Mechanism and Machine Science: Proceedings of the 15th IFToMM World Congress on Mechanism and Machine Science, vol. 15, pp. 165–174. Springer, Heidelberg (2019). https://doi.org/10.1007/978-3-030-20131-9_17
2. Chen, B., et al.: Recent developments and challenges of lower extremity exoskeletons. J. Orthop. Transl. **5**, 26–37 (2016)
3. Anam, K., Al-Jumaily, A.A.: Active exoskeleton control systems: state of the art. Procedia Eng. **41**, 988–994 (2012)
4. Díaz, I., Gil, J.J., Sánchez, E.: Lower-limb robotic rehabilitation: literature review and challenges. J. Robot. **2011**, 1–11 (2011)
5. Yan, T., Cempini, M., Oddo, C.M., Vitiello, N.: Review of assistive strategies in powered lower-limb orthoses and exoskeletons. Robot. Auton. Syst. **64**, 120–136 (2015)

6. Huo, W., Mohammed, S., Moreno, J.C., Amirat, Y.: Lower limb wearable robots for assistance and rehabilitation: a state of the art. IEEE Syst. J. **10**(3), 1068–1081 (2014)
7. Jarrassé, N., et al.: Robotic exoskeletons: a perspective for the rehabilitation of arm coordination in stroke patients. Front. Hum. Neurosci. **8**, 947 (2014)
8. Geonea, I., Ceccarelli, M., Carbone, G.: Design and analysis of an exoskeleton for people with motor disabilities. In: Proceedings of the 14th IFToMM World Congress, pp. 33–40 (2015)
9. Geonea, I.D., Tarnita, D.: Design and evaluation of a new exoskeleton for gait rehabilitation. Mech. Sci. **8**(2), 307–321 (2017)
10. Young, A.J., Ferris, D.P.: State of the art and future directions for lower limb robotic exoskeletons. IEEE Trans. Neural Syst. Rehabil. Eng. **25**(2), 171–182 (2016)
11. Wang, M.F., Ceccarelli, M., Carbone, G.: Experimental tests on operation performance of a LARM leg mechanism with 3-DOF parallel architecture. Mech. Sci. **6**(1), 1–8 (2015)
12. Li, T., Ceccarelli, M.: Design and simulated characteristics of a new biped mechanism. Robotica **33**(7), 1568–1588 (2015)
13. Wojtyra, M.: Dynamical analysis of human walking. In: 15^{th} European ADAMS Users' Conference, pp. 15–17 (2000)
14. Varela, M.J., Ceccarelli, M., Flores, P.: A kinematic characterization of human walking by using CaTraSys. Mech. Mach. Theory **86**, 125–139 (2015)